Available online at www.sciencedirect.com

SCIENCE DIRECT®

Optics Communications 245 (2005) 177–186

OPTICS COMMUNICATIONS

www.elsevier.com/locate/optcom

Comparison of fiber-based Sagnac interferometers for self-switching of optical pulses

Wen-hua Cao *, P.K.A. Wai

Photonics Research Center and Department of Electronic and Information Engineering, The Hong Kong Polytechnic University, Hung Hom, Hong Kong

Received 13 June 2004; received in revised form 27 July 2004; accepted 7 October 2004

Abstract

Self-switching of ultrashort optical pulses in a gain-distributed nonlinear amplifying fiber loop mirror (NALM) is investigated numerically in the soliton regime. Switching characteristics of this device is compared to those of the nonlinear optical loop mirror (NOLM) and the conventional NALM that uses a lumped gain. We show that, as compared with the NOLM or the conventional NALM, the gain-distributed NALM can produce higher-quality pulses and permits more efficient pulse compression. We also show that the gain-distributed NALM has several advantages over the conventional NALM such as sharpened switching edges, flattened switching peak, and robustness to gain variations.

PACS: 42.65.P; 42.81; 42.65.R
Keywords: Optical switches; Optical fibers; Nonlinear optics; Pulse compression

1. Introduction

Nonlinear optical loop mirrors (NOLMs) [1], capable of handling ultrashort pulses, have found many applications, such as soliton self-switching [1–3], all-optical demultiplexing [4], wavelength conversion [5], pulse pedestal suppression [6], and noise filtering [7] in all-optical fiber communication systems. Self-switching with the NOLM is achieved by placing a symmetry-breaking element in the loop and thereby causing counterpropagating pulses to acquire different amounts of nonlinear phase, so at recombination phase difference produce reflected and transmitted (switched) outputs. To break the symmetry, the original NOLM [1] uses an asymmetric coupler. Alternative schemes that can achieve symmetry breaking of the loop without resorting to an asymmetric coupler have been proposed and demonstrated to work. Examples include using dispersion-imbalanced fibers

* Corresponding author. Tel.: +852 2766 6209; fax: +852 2362 8439.
E-mail address: wwhhcao@163.com (W.-h. Cao).

0030-4018/$ - see front matter
doi:10.1016/j.optcom.2004.10.015

[8–10], asymmetrically induced nonlinear birefringence effects [11,12], or an asymmetrically located optical amplifier [13,14].

NOLMs with asymmetrically located optical amplifiers [13,14], also known as nonlinear amplifying loop mirrors (NALMs), best exploit the fiber nonlinearity resulting in the lowest threshold switching power. However, since the amplifier is much shorter than the fiber loop and is located close to the coupler, the counterpropagating pulses in the loop are not amplified simultaneously, i.e., one pulse is amplified just after entering the loop while the other experiences amplification just before exiting the loop. As a result, evolutions of the two pulses in the loop are quite different, especially in the soliton regime. When they recombine at the coupler, seriously mismatched pulse shapes lead to the poor quality of the switched pulses. It was predicted [15] that pulses switched by the conventional NALM that incorporates a lumped gain (hereinafter, we call it gain-lumped NALM) contain frequency chirp, which will affect signal propagation over long-distance, especially in soliton communication systems. Other problems with the gain-lumped NALM are that the switching curve is not sufficiently sharp and the switching characteristics are sensitive to gain variations.

In this paper we numerically study, for the first time to our knowledge, the self-switching characteristics of a gain-distributed NALM which is distinct to the gain-lumped NALM in that a distributed gain [16] rather than a lumped gain is uniformly placed along the loop while using an asymmetric coupler. We show that, as compared with the NOLM or the gain-lumped NALM, the gain-distributed NALM can produce higher-quality pulses and permits more efficient pulse compression. We also show that the gain-distributed NALM has several advantages over the gain-lumped NALM such as sharpened switching edges, flattened switching peak, and robustness to gain variations.

2. Basic equations

For simulations of pulse evolution in a fiber loop, we use the split-step Fourier method to solve the nonlinear Schrödinger equation including negative group-velocity dispersion (GVD), self-phase modulation (SPM), and gain or loss. In dimensionless form, the equation is

$$\mathrm{i}\frac{\partial u}{\partial \xi}+\frac{1}{2}\frac{\partial^2 u}{\partial \tau^2}+|u|^2u=\frac{\mathrm{i}}{2}\mu u, \tag{1}$$

where ξ, τ, and $u(\xi,\tau)$ denote, respectively, the normalized distance, time, and pulse envelope in soliton units. In real parameters

$$\xi=\frac{z}{L_{\mathrm{D}}}=\frac{z|\beta_2|}{T_0^2},\quad \tau=\frac{t-z/v_g}{T_0},$$
$$\mu=(g_0-\alpha)L_{\mathrm{D}}, \tag{2}$$

where T_0 is the half-width (at $1/e$-intensity point) of the input pulse, v_{g} is the group velocity, β_2 is the GVD coefficient, g_0 is the unsaturated gain, α is the attenuation constant, and $L_{\mathrm{D}}=T_0^2/|\beta_2|$ is the dispersion length. The term on the right-hand side of Eq. (1) accounts for gain or loss. Gain dispersion and higher-order effects such as Raman self-scattering (RSS) and third-order dispersion can be neglected for input pulses wider than 5 ps. We also neglect gain saturation, which is justified since we are only concerned with the switching of a single pulse with a typical energy ($\sim$1 pJ) much lower than the saturation energy of most amplifiers such as erbium-doped fiber amplifiers which is on the order of 1 μJ.

3. Self-switching characteristics of NOLM and gain-lumped NALM

Before we investigate pulse self-switching in a gain-distributed NALM, we discuss the switching characteristics of NOLM and gain-lumped NALM. In the case of NOLM, the loop is constructed from a piece of passive fiber, i.e., $g_0=0$ in Eq. (2). Fiber loss is considered with $\alpha=0.046$ km^{-1} (i.e., 0.2 dB/km). The input pulse is assumed to be $u(0,\tau)=A\,\mathrm{sech}(\tau)$ with FWHM pulsewidth of $T_{\mathrm{FWHM}}=5$ ps ($T_0\approx 2.84$ ps), where A is related to the physical parameters by

$$A^2=\frac{\gamma P_0 T_0^2}{|\beta_2|} \tag{3}$$

γ is the nonlinearity coefficient and P_0 is the peak power of the input pulse. We choose $\beta_2 = -20$ ps^2/km and $\gamma = 5$ W^{-1} km^{-1}. The loop length is fixed at πL_D ($\sim$1.26 km). In most applications [10,15–17] NOLMs or NALMs are set to operate around the first switching peak because RSS inherent in the ultrashort pulses causes the devices to fail beyond the first peak as a result of incomplete interference. So in the following most of our investigations are focused on the first switching peak. Fig. 1(a), (b), (c), and (d) shows, respectively, the switching characteristics of the NOLMs for coupler power-splitting ratios of (a) 56:44, (b) 58:42, (c) 60:40, and (d) 62:38. Where the solid, dashed, and dash-dotted curves show, respectively, the dependence of the loop transmission, the pedestal energy, and time-bandwidth product ($\Delta\nu\Delta\tau \times 100$) of the transmitted pulse on the peak power of the input pulse. The horizontal dotted line in each case shows the time-bandwidth product of 0.315(×100) of a transform-limited hyperbolic-secant pulse. Here the transmission is defined as the ratio of the transmitted (switched) energy to the sum of the transmitted and reflected energies. The pedestal energy is defined as the relative difference between the total energy of the transmitted pulse and the energy of a hyperbolic-secant pulse having the same peak power and width as those of the transmitted pulse, i.e.,

$$\text{Pedestal energy } (\%) = \frac{|E_{\text{total}} - E_{\text{sech}}|}{E_{\text{total}}} \times 100\%. \tag{4}$$

Note that the energy of a hyperbolic-secant pulse with peak power P_{peak} and pulse width T_{FWHM} is given by

$$E_{\text{sech}} = 2P_{\text{peak}} \frac{T_{\text{FWHM}}}{1.763}. \tag{5}$$

The general feature shown in Fig. 1 is that the quality of the transmitted pulses around the transmission peak are not so good howsoever the coupler power-splitting ratio is changed, because the transmitted pulses are not transform limited and are accompanied by non-negligible pedestals. Another disadvantage of the NOLM is that it requires a relatively high threshold switching power.

Fig. 2(a)–(d) shows the compression factor (solid curve) and the corresponding soliton order (dashed curve) of the transmitted pulses under conditions identical to those of Fig. 1(a), (b), (c), and (d), respectively. Where the compression factor is defined as the ratio of T_{FWHM} of the input pulse to that of the transmitted pulse and the

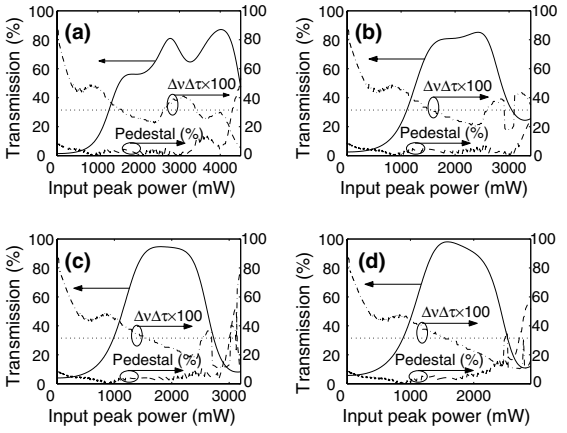

Fig. 1. Transmission, pedestal energy, and time-bandwidth product of the switched pulse as a function of the input peak power for NOLMs with coupler power-splitting ratios of (a) 56:44, (b) 58:42, (c) 60:40, and (d) 62:38. In all cases, the input pulsewidth is 5 ps (FWHM) and the loop length is fixed at πL_D ($\sim$1.26 km). The dotted curve shows the time-bandwidth product of 0.315(×100) of a transform-limited hyperbolic-secant pulse.

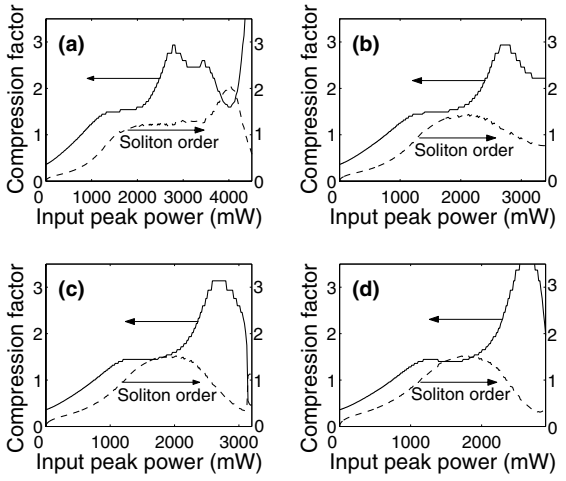

Fig. 2. Compression factor and soliton order of the switched pulses corresponding to Fig. 1(a), (b), (c), and (d), respectively.

soliton order is estimated from the peak power and width of the transmitted pulse. It is seen that, around the transmission peak, the compression factor increases slowly as the coupler power-splitting ratio approaches to 50:50 (compare Fig. 2 with Fig. 1). Although higher compression factor can be achieved near the right edge of the switching window (for example, see Fig. 2(d)), the switched energy is small and the quality of the switched pulse is poor. In practice, NOLM is set to operate around the transmission peak. Fig. 2 also shows that, in each case, the soliton orders are close to those of fundamental solitons. However, the transmitted pulses do not actually retain the characteristics of fundamental solitons because they are chirped and are accompanied by pedestals (see Fig. 1). These features will be compared to those of the gain-distributed NALM in Section 4.

The threshold switching power of the NOLM can be significantly lowered by inserting an optical amplifier at one end of the loop [13,14]. Fig. 3(a) and (b) shows the dependence of the loop transmission, the pedestal energy and time-bandwidth product ($\Delta\nu\Delta\tau \times 100$) of the transmitted pulse on the input peak power under conditions identical to those of Fig. 1 except that the coupler is symmetric with a power-splitting ratio of 50:50 and that an amplifier with gain of (a) 5 and (b) 10 dB, respectively, is placed within the loop immediately after the coupler. The amplifier length is assumed to be much shorter than the loop length, which is the reason we call the device gain-lumped NALM. We see that, as compared with the NOLM, the switching power is significantly reduced. This is because the presence of the amplifier increases the SPM induced relative phase shift between the counterpropagating pulses in the loop, leading to improved exploitation of loop nonlinearity. However, as compared with the NOLM, the gain-lumped NALM exhibits slow switching transitions near the switching edges, which is a disadvantage for ultrafast all-optical signal processing. The quality of the transmitted pulse is also poor which will be explained in Section 4. Fig. 3(c) and (d) shows the compression factor (solid curve) and the corresponding soliton order (dashed curve) of the transmitted pulses under conditions identical to those of Fig. 3(a) and (b), respectively. As in the case of NOLM, pulse compression provided by gain-lumped NALM is not efficient.

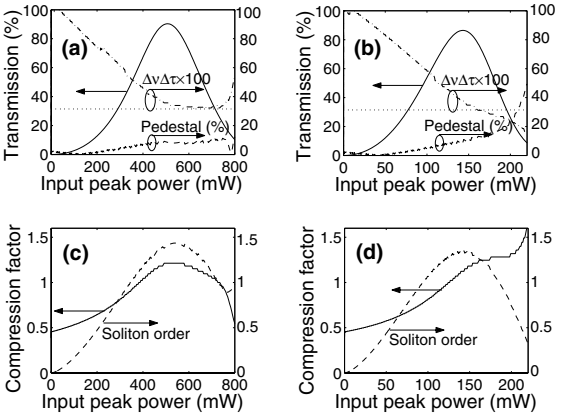

Fig. 3. Transmission, pedestal energy, and time-bandwidth product of the switched pulse as a function of the input peak power for gain-lumped NALMs with gains of (a) 5 and (b) 10 dB, respectively. (c) and (d) show the compression factor and soliton order of the switched pulses corresponding to (a) and (b), respectively.

4. Gain-distributed NALM and its comparison to NOLM and gain-lumped NALM

Fig. 4(a)–(d) shows the switching characteristics of the gain-distributed NALM for coupler power-splitting ratios of (a) 54:46, (b) 55:45, (c) 56:44, and (d) 57:43. In each case a 10-dB gain is uniformly distributed along the loop, and the loop length, the loop parameters β_2 and γ, and the input pulsewidth are fixed as before. As compared with the cases of NOLM (Fig. 1) or gain-lumped NALM (Fig. 3(a) and (b)), we can see that distributed gain causes a significant improvement in the quality of the transmitted pulse. Here, the pedestals of the transmitted pulses are very small (less than 5%) and the transmitted pulses are very close to transform-limited pulses. In addition, distributed gain also causes a significant sharpening of the switching transition as well as a flattening of the switching peak as compared with the case of gain-lumped NALM.

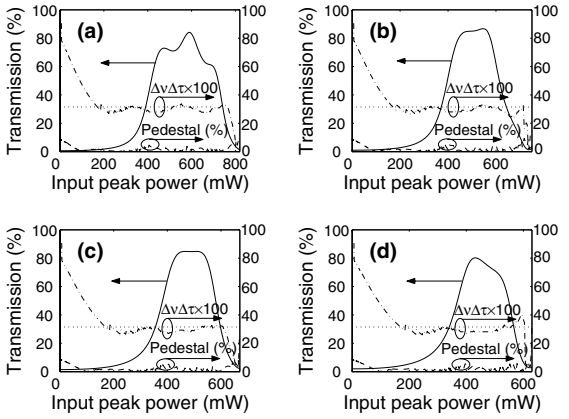

Fig. 4. Transmission, pedestal energy, and time-bandwidth product of the switched pulse as a function of the input peak power for gain-distributed NALMs with coupler power-splitting ratios of (a) 54:46, (b) 55:45, (c) 56:44, and (d) 57:43. In all cases a 10-dB gain is uniformly distributed along the loop, and the loop length and the input pulsewidth are fixed and are identical to those used for Figs. 1–3.

Fig. 5(a)–(d) shows the compression factor and the soliton order of the transmitted pulses under conditions identical to those of Fig. 4(a), (b), (c), and (d), respectively. It is seen that the gain-distributed NALM permits more efficient pulse compression than the NOLM or the gain-lumped NALM. The soliton orders of the transmitted pulses around the transmission peaks are close to those of fundamental solitons. Note that, since pulses transmitted form the gain-distributed NALM have negligible pedestals and are nearly chirp free, they are more close to fundamental solitons than those from the NOLM or the gain-lumped NALM.

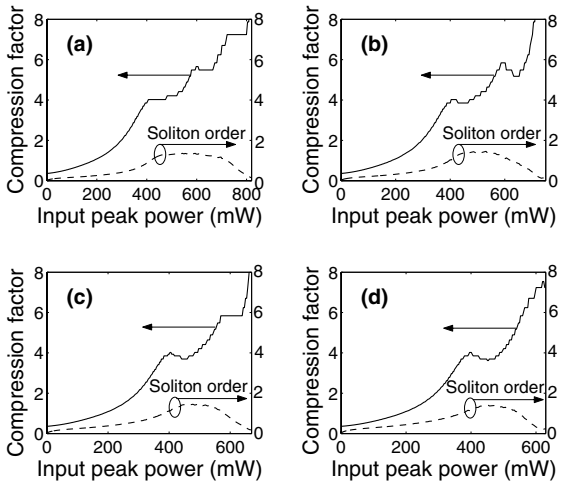

Fig. 5. Compression factor and soliton order of the switched pulses corresponding to Fig. 4(a), (b), (c), and (d), respectively.

The above studies assume that the gain around the loop is uniform and is the same in the two directions. This implies that the pump wave should be uniform along the loop and pump depletion can be neglected. To avoid asymmetric coupling of the pump beam, one may place two additional couplers inside the loop, both of which are located near the main coupler. The pump beam may be coupled into the loop through one and come out from the other. To reduce the effect of pump depletion on the switching performance of the device (because the loop is relatively long), one may pump the loop simultaneously in both clockwise and counterclockwise directions.

The pulse compression nature of the gain-distributed NALM is useful for soliton regeneration in long-distance soliton-based communication systems. In such systems fiber loss degrades soliton energy and, when the energy is lower than that of a fundamental soliton, dispersion broadens the pulse width. By using the distributed NALM, we can simultaneously compensate for the loss induced energy degradation and dispersion-induced pulsewidth broadening and suppress background dispersive waves [17] without the use of any dispersion compensation elements.

More efficient pulse compression can be achieved with gain-distributed NALM when it operates at the subsequent switching peaks. Fig. 6(a) shows the multiple-peaked switching of the gain-distributed NALM under conditions identical to those of Fig. 4(c), which is possible by using relatively long pulses to suppress RSS [18]. Where the dashed curve represents the pedestal and the dash-dotted curve represents the compression factor. We see that compression factors of 5, 8, and 10 can be achieved at the first, second, and third peaks, respectively. The pedestal around each peak is small and the on–off switching contrast is nearly the same for all peaks. For comparison Fig. 6(b) and (c) show the multiple-peaked switching of

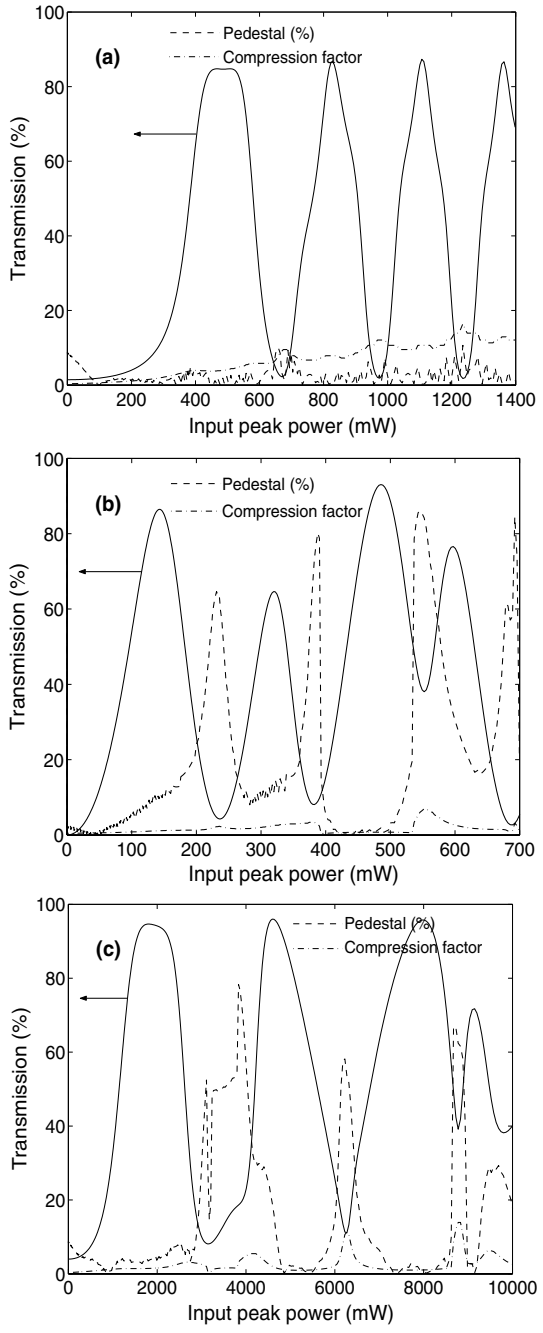

Fig. 6. (a) Multiple-peaked switching of the gain-distributed NALM under conditions identical to those of Fig. 4(c), (b) multiple-peaked switching of the gain-lumped NALM under conditions identical to those of Fig. 3(b), and (c) multiple-peaked switching of the NOLM under conditions identical to those of Fig. 1(c).

the gain-lumped NALM and NOLM under conditions identical to those of Figs. 3(b) and 1(c), respectively. It is seen that, in both cases, the compression factor around all the transmission peaks is kept below 3. The reason is that, when the NOLM or the gain-lumped NALM operate at the higher switching peaks, pulse evolution in the loop is so complex because of higher-order soliton formation such that high transmission and high compression factor cannot be achieved simultaneously.

The different switching characteristics between the gain-distributed NALM and the NOLM (or the gain-lumped NALM) can be understood as follows. In the case of NOLM, the pulses propagate along the loop are higher-order solitons which exhibit complex pulse shaping during their evolutions. The evolutions of clockwise and counterclockwise pulses are different because of the asymmetric coupler. As a result, serious mismatch of pulse shapes occurs when the two pulses recombine at the coupler. Fig. 7(a) shows the clockwise (solid curve) and counterclockwise (dashed curve) pulse shapes after they travel around the loop but before recombination at the coupler under conditions identical to those corresponding to the transmission peak of Fig. 1(c). Where the intensity is normalized to the peak intensity of the input pulse. The shape of the transmitted pulse is given by the dashed–dotted curve. We see that the clockwise and counterclockwise pulses are seriously mismatched in shape when they interfere at the coupler. The situation is even worse for the gain-lumped NALM as shown in Fig. 7(b), where the conditions are identical to those corresponding to the transmission peak of Fig. 3(b). Since the amplifier is located close to the coupler in this case, the clockwise and counterclockwise pulses are not amplified simultaneously and their evolutions along the loop are different, i.e., one experiences compression and the other experiences broadening. Mismatched pulse shapes lead to incomplete interference at the coupler and thus the poor quality of the transmitted pulses. However, the situation is different for the gain-distributed NALM as shown in Fig. 7(c), where the conditions are identical to those corresponding to the transmission peak of Fig. 4(c). In this case, both the

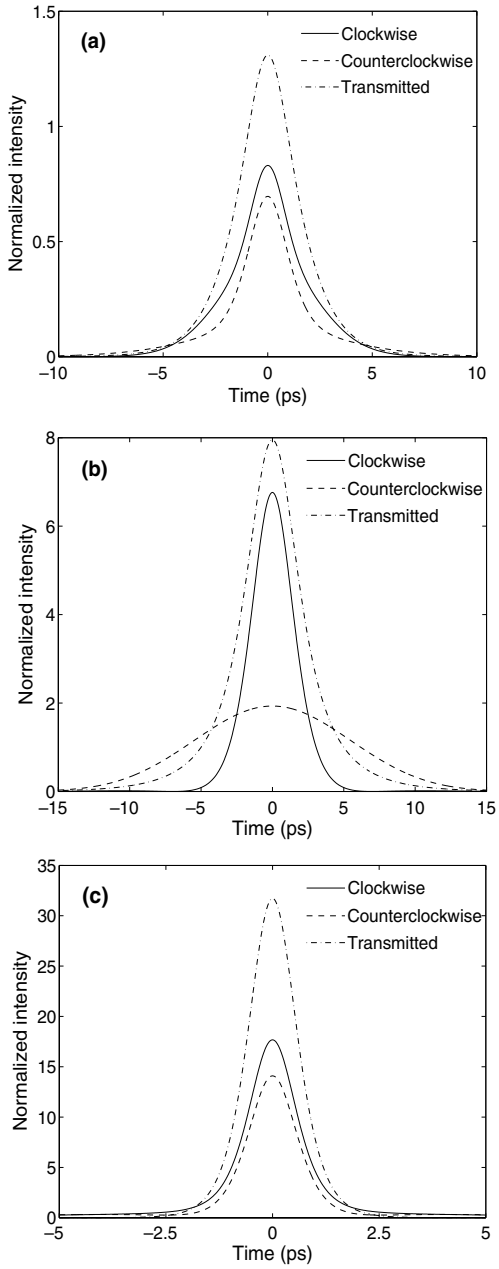

Fig. 7. Temporal pulse shapes of the clockwise and counterclockwise traveling pulses before they interfere at the coupler for (a) NOLM under conditions identical to those corresponding to the transmission peak of Fig. 1(c), (b) gain-lumped NALM under conditions identical to those corresponding to the transmission peak of Fig. 3(b), and (c) gain-distributed NALM under conditions identical to those corresponding to the transmission peak of Fig. 4(c). The shapes of the transmitted pulses are given by the dashed–dotted curves.

clockwise and counterclockwise pulses experience compression because of the distributed gain. Amplification of the two pulses is nearly adiabatic [19,20], i.e., during the amplification process their energies remain localized in the amplified pulses which adjust their shapes and widths as they propagate along the loop such that they approach to fundamental solitons. Thus, unlike the cases of the NOLM or the gain-lumped NALM, serious mismatch of the counterpropagating pulse shapes in the gain-distributed NALM is prevented, leading to more complete interference when the two pulses recombine at the coupler.

5. Effect of loop length

In the above discussions we have assumed a fixed loop length of πL_D ($\sim$1.26 km) for the three types of interferometric switches. In this Section, we study the effect of varying the loop length on the switching characteristics of these devices. Fig. 8(a)–(d) shows the switching characteristics of the gain-distributed NALM for loop lengths of (a) πL_D, (b) $3\pi L_D/4$, (c) $\pi L_D/2$, and (d) $\pi L_D/4$. In each case a 10-dB gain is uniformly distributed along the loop, the coupler power-splitting ratio is fixed at 56:44, and the loop parameters (β_2 and

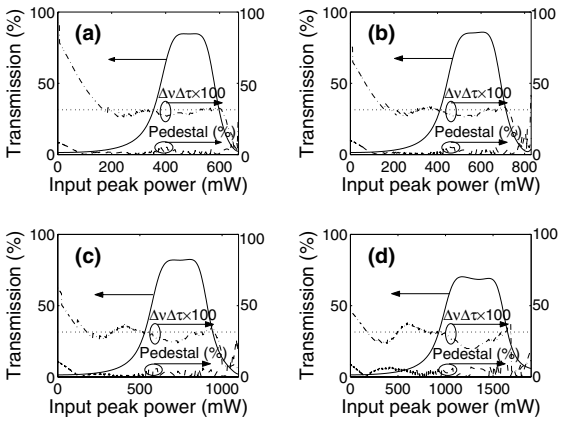

Fig. 8. Switching characteristics of the gain-distributed NALMs with loop lengths of (a) πL_D, (b) $3\pi L_D/4$, (c) $\pi L_D/2$, and (d) $\pi L_D/4$. In each case a 10-dB gain is uniformly distributed along the loop and the coupler power-splitting ratio is fixed at 56:44.

γ) and the input pulsewidth are fixed as before. The main feature is that decreasing the loop length leads to deterioration of the switched pulse quality, i.e., pedestal energy increases and the pulse becomes chirped. This can be easily understood. As the loop length decreases, the gain parameter μ increases (see Eqs. (1) and (2)). As a result, the condition for adiabatic amplification is not satisfied, leading to incomplete interference when the two pulses recombine at the coupler.

Decreasing the loop length also influences the performances of the gain-lumped NALM and NOLM. Figs. 9 and 10 show, respectively, the switching characteristics of the gain-lumped NALM and the NOLM for loop lengths of (a) πL_D, (b) $3\pi L_D/4$, (c) $\pi L_D/2$, and (d) $\pi L_D/4$. Where the gain is fixed at 10-dB for the gain-lumped NALMs which have a symmetric coupler, and a same coupler power-splitting ratio of 60:40 is assumed for the NOLMs. In all cases, the loop parameters (β_2 and γ) and the input pulsewidth are fixed as before. As compared with the case of the gain-distributed NALM, we see that the quality of the transmitted pulses from the NOLM is more sensitive to loop length. The reason is as follows. In the case of NOLM, the threshold switching power increases rapidly as the loop length is decreased. Thus, the soliton orders of both the clockwise and counterclockwise pulses are increased and pulse evolution in the NOLM becomes more and more complex. Mismatch of the counterpropagating pulse shapes in the NOLM is more serious than in the other two devices.

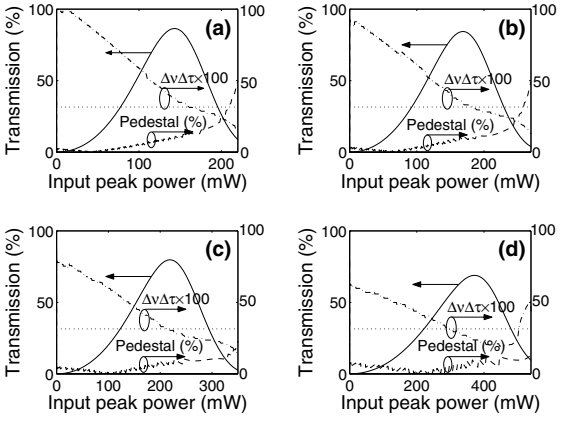

Fig. 9. Switching characteristics of the gain-lumped NALMs with loop lengths of (a) πL_D, (b) $3\pi L_D/4$, (c) $\pi L_D/2$, and (d) $\pi L_D/4$. The gain is fixed at 10-dB for each case.

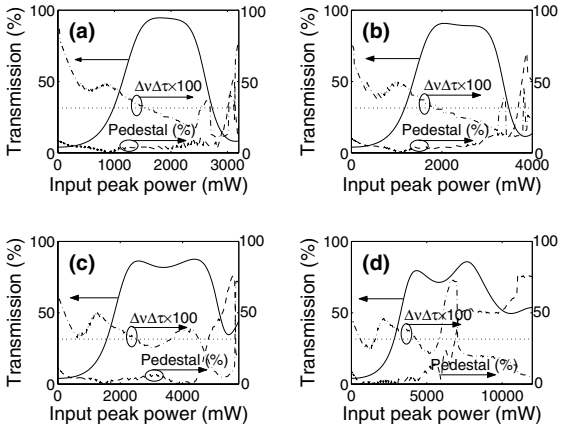

Fig. 10. Switching characteristics of the NOLMs with loop lengths of (a) πL_D, (b) $3\pi L_D/4$, (c) $\pi L_D/2$, and (d) $\pi L_D/4$. The coupler power-splitting ratio is fixed at 60:40 for each case.

6. Effect of gain variation

Thus far, we assumed that the total gain of the gain-distributed NALM or the gain-lumped NALM remains unchanged during the switching process. In some cases, gain may be time dependent because of pump power fluctuation or amplifier gain saturation which cannot be neglected if the repetition rate of the incident pulses is very high. In this final Section, we investigate how gain variation affects the switching performance of the two devices. For both cases, the loop length is fixed at πL_D and the incident pulsewidth is fixed as before. The peak power of the incident pulse is fixed at 143 mW for the gain-lumped NALM and at 465 mW for the gain-distributed NALM, which correspond to the transmission peaks of Figs. 3(b) and 4(c), respectively. Only gain is varied around 10 dB for both cases. Fig. 11(a), (b), (c), and (d) shows, respectively, the transmission, pedestal energy, time-bandwidth product, and compression factor of the transmitted pulses as a function of gain. The solid and dashed curves represent, respectively, the cases of gain-distributed

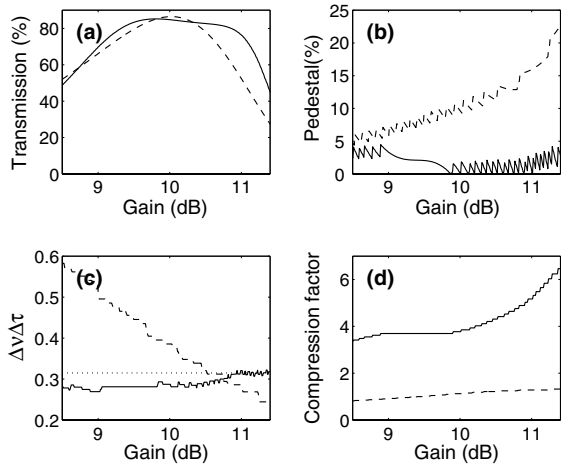

Fig. 11. Influence of gain variation on the switching characteristics of the gain-lumped NALM (dashed curves) and the gain-distributed NALM (solid curves). For both cases, the loop length is fixed at πL_D and the incident pulsewidth is fixed as before. The peak power of the incident pulse is fixed at 143 mW for the gain-lumped NALM and at 465 mW for the gain-distributed NALM.

NALM and gain-lumped NALM. We see that, in comparison with the gain-lumped NALM, the transmission of the gain-distributed NALM is relatively flat and wide over a range of gain. In addition, the pedestal energy and time-bandwidth product of the gain-distributed NALM are also less sensitive to gain variation. This implies that the switching characteristics of the gain-distributed NALM will be less affected by amplifier gain saturation than that of the gain-lumped NALM if gain saturation cannot be neglected. The reason is as follows: In the case of gain-lumped NALM, gain variation only affects the nonlinear phase shift of the clockwise pulse (we assumed that the lumped amplifier is located near the coupler such that the clockwise pulse experiences amplification earlier than the counterclockwise pulse). In the case of the gain-distributed NALM however gain variation has nearly the same influence on the nonlinear phase shifts of both the clockwise and counterclockwise pulses. Thus, the difference of the nonlinear phase shift (which is required for switching) between the counterpropagating pulses in the gain-distributed NALM is less affected than that in the case of gain-lumped NALM, leading to robustness of the gain-distributed NALM to gain variation.

7. Conclusion

In conclusion, we have analyzed the switching characteristics of a NALM with distributed gain and compared it to the NOLM and the conventional NALM with lumped gain. We show that, as compared with the NOLM or the conventional NALM, the NALM with distributed gain can produce higher-quality pulses and permits more efficient pulse compression. Furthermore, the NALM with distributed gain has additional advantages over the conventional NALM such as sharpened switching edges, flattened switching peak, and robustness to gain variations.

Acknowledgments

This work was supported by the Research Grant Council of the Hong Kong Special Administrative Region of China under Project PolyU5242/03E, by the National Natural Science Foundation of China under Project 60277016, and by the Guangdong Natural Science Foundation of China under Project 021357.

References

[1] N.J. Doran, D. Wood, Opt. Lett. 13 (1988) 56.
[2] K.J. Blow, N.J. Doran, B.K. Nayar, Opt. Lett. 14 (1989) 754.
[3] M.N. Islam, E.R. Sunderman, R.H. Stolen, W. Pleibel, J.R. Simpson, Opt. Lett. 14 (1989) 811.
[4] K.J. Blow, N.J. Doran, B.P. Nelson, Electron. Lett. 26 (1990) 962.
[5] K.J. Blow, N.J. Doran, B.K. Nayar, B.P. Nelson, Opt. Lett. 15 (1990) 248.
[6] K. Smith, N.J. Doran, P.G.J. Wigley, Opt. Lett. 15 (1990) 1294.
[7] N.J. Smith, N.J. Doran, J. Opt. Soc. Am. B 12 (1995) 1117.
[8] A.L. Steele, J.P. Hemingway, Opt. Commun. 123 (1996) 487.
[9] W.S. Wong, S. Namiki, M. Margalit, H.A. Haus, E.P. Ippen, Opt. Lett. 22 (1997) 1150.

[10] K.R. Tamura, M. Nakazawa, IEEE Photon. Technol. Lett. 13 (2001) 526.
[11] E.A. Kuzin, J.A. Andrade-Lucio, B.I. Escamilla, R. Rojas-Laguna, J. Sanchez-Mondragon, Opt. Commun. 144 (1997) 60.
[12] H.Y. Rhy, B.Y. Kim, H.W. Lee, IEEE J. Quantum Electron. 36 (2000) 89.
[13] M.E. Fermann, F. Haberl, M. Hofer, H. Hochreiter, Opt. Lett. 15 (1990) 752.
[14] D.J. Richardson, R.I. Laming, D.N. Payne, Electron. Lett. 26 (1990) 1779.
[15] E. Yamada, M. Nakazawa, IEEE J. Quantum Electron. 30 (1994) 1842.
[16] W. Cao, P.K.A. Wai, Opt. Lett. 28 (2003) 284.
[17] I. Gabitov, D.D. Holm, B.P. Luce, J. Opt. Soc. Am. B 14 (1997) 1850.
[18] D.A. Pattison, W. Forysiak, P.N. Kean, I. Bennion, N.J. Doran, Opt. Lett. 20 (1995) 19.
[19] W. Hodel, J. Schutz, H.P. Weber, Opt. Commun. 88 (1992) 173.
[20] M. Nakazawa, K. Kurokawa, H. Kubota, K. Suzuki, Y. Kimura, Appl. Phys. Lett. 57 (1990) 653.